Hindawi
Discrete Dynamics in Nature and Society
Volume 2019, Article ID 3149602, 6 pages
https://doi.org/10.1155/2019/3149602

Research Article

Shrinkage Points of Golden Rectangle, Fibonacci Spirals, and Golden Spirals

Jun-Sheng Duan

School of Sciences, Shanghai Institute of Technology, Shanghai 201418, China

Correspondence should be addressed to Jun-Sheng Duan; duanjs@sit.edu.cn

Received 25 June 2019; Revised 11 November 2019; Accepted 6 December 2019; Published 20 December 2019

Academic Editor: Cengiz Çinar

Copyright © 2019 Jun-Sheng Duan. This is an open access article distributed under the Creative Commons Attribution License, which permits unrestricted use, distribution, and reproduction in any medium, provided the original work is properly cited.

We investigated the golden rectangle and the related Fibonacci spiral and golden spiral. The coordinates of the shrinkage points of a golden rectangle were derived. Properties of shrinkage points were discussed. Based on these properties, we conduct a comparison study for the Fibonacci spiral and golden spiral. Their similarities and differences were looked into by examining their polar coordinate equations, polar radii, arm-radius angles, and curvatures. The golden spiral has constant arm-radius angle and continuous curvature, while the Fibonacci spiral has cyclic varying arm-radius angle and discontinuous curvature.

1. Introduction

A golden rectangle is such one that if we cut off a square section whose side is equal to the shortest side, the piece that remains has the same ratio of side lengths with the original rectangle.

Let a golden rectangle has the side lengths a and b ($b < a$), then the ratio $\lambda = b/a$ satisfies

$$\lambda = \frac{b}{a} = \frac{a-b}{b} = \frac{1-b/a}{b/a} = \frac{1-\lambda}{\lambda}, \tag{1}$$

that is

$$\lambda^2 = 1 - \lambda. \tag{2}$$

Its positive root is the golden ratio:

$$\lambda = \frac{\sqrt{5}-1}{2} \approx 0.618. \tag{3}$$

The golden ratio is also known as the golden section, golden proportion, and golden mean [1]. The golden ratio has been found incorporated almost in all natural or organic structures, such as the bone structure of human beings [2–4], the seed pattern and geometry of plants [5], the spiral of a sea shell [6], and spiral galaxy [7]. The golden ratio was found in art and architecture as it produces pleasing shapes [8], even in special relativity [9]. Also, the golden ratio and the golden section method were applied to optimal design and search problems in different fields [10–13].

As a development of the Fibonacci numbers, Stakhov and Rozin [1, 14] proposed new continuous functions based on the golden ratio: the symmetric Fibonacci sine and cosine, symmetric Lucas sine and cosine, and quasisine Fibonacci function. In particular, a new equation of the three-dimensional surface, golden shofar, was presented in [14]. These concepts may lead to new cosmological theories [14]. In [15], the relation between Fibonacci sequences with arbitrary initial numbers and the damped oscillation equation was established.

A golden rectangle has the golden ratio of side lengths. It has been applied to the fields of architecture, drawing, photography, etc., as a representative of art beauty [8, 16]. In Section 2, we consider the shrinkage points of a golden rectangle and their properties. In Section 3, we compare the Fibonacci spiral and golden spiral, including their equations, polar radii, arm-radius angles, and curvatures.

We note that in some references, the value $1/\lambda$ is called the golden ratio and denoted as φ. Throughout this paper, we use λ to denote the golden ratio $(\sqrt{5}-1)/2$.

2. Shrinkage Points of Golden Rectangle

From the golden rectangle $OACB$ in Figure 1, the square is cut on the right, and the remaining rectangle is also a golden rectangle. We continue the operation as the following . The squares on the top, left and bottom are cut away in the follow-up three procedures. The cutting process in the counterclockwise direction can be ongoing. By the theorem of interval nest, there is a singleton (x_s, y_s), denoted by a dot in Figure 1, belonging to all of the golden rectangles. We call this singleton the shrinkage point of the original golden rectangle.

Next, we determine the location of the shrinkage point on the golden rectangle $OACB$ in Figure 1. Set up the rectangular coordinate system OAB. Points A and B have the coordinates a and b on axes OA and OB, respectively. Dashed lines represent the cut lines. Successively, they cut the axis OA at the points $d_1, c_1, d_2, c_2, \ldots$. The coordinate values are calculated as

$$\begin{aligned} c_1 &= \lambda(1-\lambda)a, \\ d_1 - c_1 &= (1-\lambda)^2 a, \\ c_2 &= \lambda(1-\lambda)a + \lambda(1-\lambda)^3 a, \\ d_2 - c_2 &= (1-\lambda)^4 a, \\ c_3 &= \lambda(1-\lambda)a + \lambda(1-\lambda)^3 a + \lambda(1-\lambda)^5 a, \ldots. \end{aligned} \tag{4}$$

By induction, we have the general expression as follows:

$$\begin{aligned} c_n &= \lambda(1-\lambda)a\left[1 + (1-\lambda)^2 + (1-\lambda)^4 + \cdots + (1-\lambda)^{2(n-1)}\right] \\ &= \lambda(1-\lambda)a\frac{1-(1-\lambda)^{2n}}{1-(1-\lambda)^2}. \end{aligned} \tag{5}$$

The limitation leads to the abscissa of the shrinkage point:

$$x_s = \lim_{n\longrightarrow\infty} c_n = \frac{1-\lambda}{2-\lambda}a. \tag{6}$$

Inserting the value of λ, it has the form

$$x_s = \frac{5-\sqrt{5}}{10}a \approx 0.276a. \tag{7}$$

Similarly, the vertical coordinate of the shrinkage point is

$$y_s = \frac{1-\lambda}{2-\lambda}b = \frac{5-\sqrt{5}}{10}b \approx 0.276b. \tag{8}$$

About the shrinkage point, we prove the following properties:

Property 1. In the golden rectangle $OACB$ in Figure 2, the points O and C are connected, and the vertical line is made such that $BS \perp OC$ with the foot point S; then, the point S is just the shrinkage point.

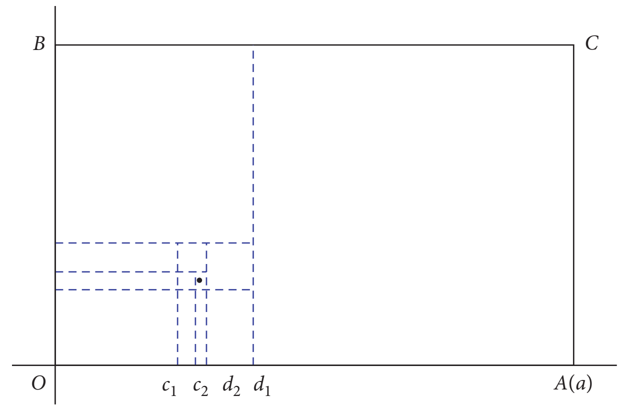

Figure 1: Shrinkage point of golden rectangle.

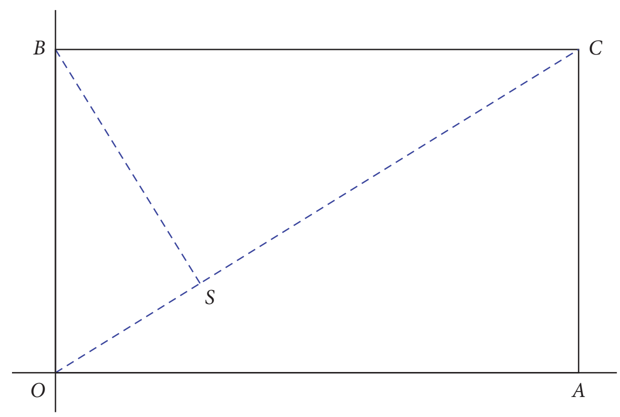

Figure 2: Geometric approach of the shrinkage point.

Proof. We suppose $OA = a$ and $OB = b = \lambda a$. Set up the rectangular coordinate system OAB. Then, the equations of straight lines OC and BS are

$$\begin{aligned} y &= \lambda x, \\ y &= -\frac{1}{\lambda}x + b, \end{aligned} \tag{9}$$

respectively. Solving the equations and using the relation $\lambda^2 = 1 - \lambda$, we obtain

$$\begin{aligned} x &= \frac{1-\lambda}{2-\lambda}a, \\ y &= \frac{1-\lambda}{2-\lambda}b. \end{aligned} \tag{10}$$

From equations (6) and (8), the proof is completed. □

Property 2. Let in Figure 3, $OACB$ be a golden rectangle and S be the shrinkage point, and $CE = CA$, $SF//OA$. Then, $SE \perp SA$, $SE/SA = \lambda$, and $\angle FSA \coloneqq \alpha = \arctan(2\lambda - 1)$.

Proof. Denote $OA = a$. Set up the Cartesian coordinate system OAB. Then, we have the following rectangular coordinates:

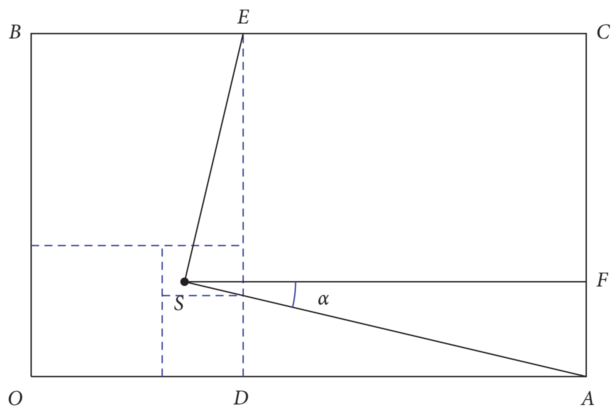

FIGURE 3: The schematic diagram for Property 2.

$$\begin{aligned} &A(a, 0), \\ &E(a - a\lambda, a\lambda), \\ &S(x_s, y_s), \\ &F(a, y_s). \end{aligned} \tag{11}$$

Considering the vectors

$$\begin{aligned} \overrightarrow{SE} &= (a - a\lambda - x_s, a\lambda - y_s), \\ \overrightarrow{SA} &= (a - x_s, -y_s), \end{aligned} \tag{12}$$

and calculating the scalar product

$$\overrightarrow{SE} \cdot \overrightarrow{SA} = (a - a\lambda - x_s)(a - x_s) - y_s(a\lambda - y_s), \tag{13}$$

yields

$$\overrightarrow{SE} \cdot \overrightarrow{SA} = 0. \tag{14}$$

This means $\overrightarrow{SE} \perp \overrightarrow{SA}$. From

$$\begin{aligned} |\overrightarrow{SE}| &= \sqrt{(a - a\lambda - x_s)^2 + (a\lambda - y_s)^2}, \\ |\overrightarrow{SA}| &= \sqrt{(a - x_s)^2 + y_s^2}, \end{aligned} \tag{15}$$

we calculate that

$$\frac{|\overrightarrow{SE}|}{|\overrightarrow{SA}|} = \lambda. \tag{16}$$

Finally, the acute angle $\angle FSA$ satisfies

$$\tan \angle FSA = \frac{y_s}{a - x_s} = 2\lambda - 1. \tag{17}$$

So, we have

$$\angle FSA \coloneqq \alpha = \arctan(2\lambda - 1). \tag{18}$$

□

In Section 3, the values of x_s, y_s, and α will be used. The length of the long side of a golden rectangle is denoted as a.

By symmetry of rectangles, there are four shrinkage points on a golden rectangle, shown by dots in Figure 4. As a comparison, we display the trisection lines and the golden lines of the same golden rectangle. The golden lines divide the width or the height at the golden ratio. These dots and lines are important references for drawing and photography.

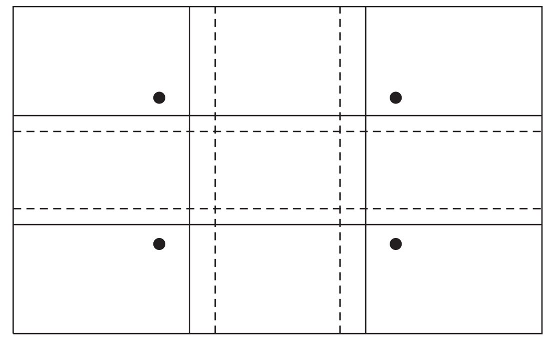

FIGURE 4: The shrinkage points, trisection lines (solid lines), and golden lines (dashed lines) of a golden rectangle.

3. Fibonacci Spirals and Golden Spirals

In this section, the shrinkage point in the lower left of a golden rectangle is served as the pole of the polar coordinate system and the origin of the rectangular coordinate system whenever a coordinate system is introduced in a golden rectangle.

3.1. Equations. The Fibonacci spiral can be generated from a golden rectangle $PACB$ in Figure 5. It is made of quarter-circles tangent to the interior of each square as follows. We draw the quarter-circle $\widehat{AE}$, center D, through two corners of the square $DACE$ such that the sides of the square are tangent to the arc. Succeedingly, the quarter-circle $\widehat{EG}$ with the center F in the square $GFEB$, the quarter-circle $\widehat{GI}$ with the center H in the square $PIHG$, the quarter-circle $\widehat{IK}$ with the center J in the square $IDKJ$, and so on.

For the sake of following comparison with the golden spiral, we derive the equation in polar coordinates for the Fibonacci spiral.

First, for the arc $\widehat{AE}$, we take a point on it with the polar coordinates $M(r, \theta)$. The ordinary rectangle coordinates are $M(r\cos\theta, r\sin\theta)$. The center of the arc has the rectangle coordinates $D(a - a\lambda - x_s, -y_s)$. According to definition, the distance is a constant, $MD = a\lambda$, i.e.,

$$(r\cos\theta - a + a\lambda + x_s)^2 + (r\sin\theta + y_s)^2 = a^2\lambda^2. \tag{19}$$

It is rearranged in the powers of r as

$$r^2 + \frac{2a\lambda^3}{2-\lambda}(\sin\theta - \lambda\cos\theta)r - \frac{\lambda^2(6\lambda - 2)}{(2-\lambda)^2}a^2 = 0. \tag{20}$$

The positive root of r is the equation in polar coordinates for the arc $\widehat{AE}$:

$$\begin{aligned} r = &-\frac{a\lambda^3}{2-\lambda}(\sin\theta - \lambda\cos\theta) \\ &+ \frac{a\lambda}{2-\lambda}\sqrt{\lambda^4(\sin\theta - \lambda\cos\theta)^2 + 6\lambda - 2}, \quad -\alpha \le \theta \le -\alpha + \frac{\pi}{2}. \end{aligned} \tag{21}$$

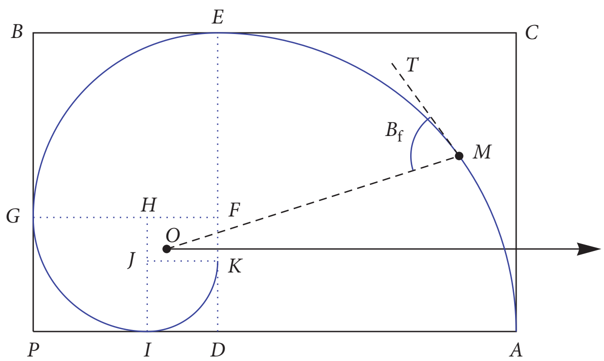

Figure 5: The Fibonacci spiral.

Polar coordinate equations for other quarter-circles can be given by similarity. For example, for the quarter-circle $\widehat{EG}$,

$$r = -\frac{a\lambda^4}{2-\lambda}\left(\sin\left(\theta-\frac{\pi}{2}\right) - \lambda\cos\left(\theta-\frac{\pi}{2}\right)\right) + \frac{a\lambda^2}{2-\lambda}\sqrt{\lambda^4\left(\sin\left(\theta-\frac{\pi}{2}\right) - \lambda\cos\left(\theta-\frac{\pi}{2}\right)\right)^2 + 6\lambda - 2}, \quad -\alpha + \frac{\pi}{2} \le \theta \le -\alpha + \pi, \tag{22}$$

and for the quarter-circle $\widehat{GI}$,

$$r = -\frac{a\lambda^5}{2-\lambda}\left(\sin(\theta-\pi) - \lambda\cos(\theta-\pi)\right) + \frac{a\lambda^3}{2-\lambda}\sqrt{\lambda^4\left(\sin(\theta-\pi) - \lambda\cos(\theta-\pi)\right)^2 + 6\lambda - 2}, \quad -\alpha + \pi \le \theta \le -\alpha + \frac{3\pi}{2}. \tag{23}$$

The Fibonacci spiral does not have continuous curvature, and is an approximation for the golden spiral. The golden spiral is a special type of the logarithmic spiral. Using the polar coordinates the logarithmic spiral has the equation:

$$r = ce^{k\theta}, \quad c > 0,\ k < 0. \tag{24}$$

The golden spiral has the special property such that for every increment $\pi/2$ of θ, the distance from the center of the spiral multiplies the golden ratio λ. That is,

$$e^{k\pi/2} = \lambda. \tag{25}$$

It follows that

$$k = \frac{2}{\pi}\ln\lambda. \tag{26}$$

The polar coordinate equation of the golden spiral is derived as follows:

$$r = ce^{((2/\pi)\ln\lambda)\theta}, \tag{27}$$

or equivalently,

$$r = c\lambda^{(2/\pi)\theta}. \tag{28}$$

In the golden rectangle $PACB$ in Figure 6, since the modulus of the vector $\overrightarrow{OA}$ is

$$|\overrightarrow{OA}| = \sqrt{(a-x_s)^2 + y_s^2} = \frac{a}{2-\lambda}\sqrt{1+\lambda^6}, \tag{29}$$

and the intersection angle between the polar axis and vector $\overrightarrow{OA}$ is $\alpha = \arctan(2\lambda - 1)$, we have the following property.

Property 3. In the golden rectangle $PACB$ in Figure 6, the golden spiral with the shrinkage point O as the pole, through the point A can be given by the equation:

$$r = \frac{a}{2-\lambda}\sqrt{1+\lambda^6}\,\lambda^{(2/\pi)(\theta+\alpha)}. \tag{30}$$

In Figure 6, we show the Fibonacci spiral in solid line and golden spiral in dashed line. In order to display their distinction, the difference of polar radii of the Fibonacci spiral and golden spiral, $r_f - r_g$, is plotted in the ordinary rectangle coordinate system in Figure 7, where we take $a = 1$. In Figure 6, the two spirals overlap at each corners $A, E, G, I, \ldots$. Within each of quarter-circles, the two spirals intersect exactly once.

3.2. Arm-Radius Angles. The arm-radius angle at a point M on a spiral is the acute angle between the tangent line at the point M and the polar radius OM. It is well known that for the logarithmic spiral $r = ce^{k\theta}, c > 0, k < 0$, the arm-radius angle is constant, and it satisfies $\cot\beta = -k$. So, the logarithmic spiral is also called equiangular spiral. As a special case of logarithmic spiral, the golden spiral $r = ce^{((2/\pi)\ln\lambda)\theta}$ has the equiangular property, i.e., the arm-radius angle, independent of c and θ:

$$\beta_g = \operatorname{arccot}\left(-\frac{2}{\pi}\ln\lambda\right) \approx 1.2735\ \text{radian (or } 72.97^\circ\text{)}, \tag{31}$$

as shown in Figure 8.

For the Fibonacci spiral in Figure 5, the arm-radius angle β_f is not constant, but periodic variation such that $\beta_f(\theta + (\pi/2)) = \beta_f(\theta)$ by similarity. For the quarter-circle $\widehat{AE}$ in Figure 5, the parameter equation is

$$\begin{cases} x = r(\theta)\cos\theta, \\ y = r(\theta)\sin\theta, \end{cases} \tag{32}$$

where $r(\theta)$ is given in equation (21). From the vectors

$$\overrightarrow{OM} = (r(\theta)\cos\theta, r(\theta)\sin\theta), \quad \overrightarrow{MT} = (x'(\theta), y'(\theta)), \tag{33}$$

we express the arm-radius angle for the Fibonacci spiral:

$$\beta_f = \arccos\frac{|\overrightarrow{OM}\cdot\overrightarrow{MT}|}{|\overrightarrow{OM}|\cdot|\overrightarrow{MT}|}, \quad -\alpha \le \theta \le \frac{\pi}{2} - \alpha. \tag{34}$$

The arm-radius angle β_f is a complicated function of θ, independent of a. By means of the software MATHEMATICA, the curves of arm-radius angles β_f and β_g versus polar

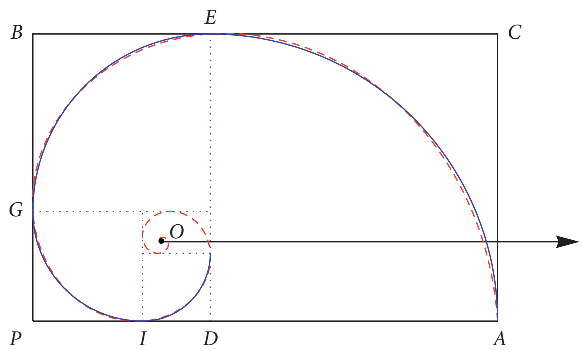

Figure 6: The Fibonacci spiral (solid line) and golden spiral (dashed line).

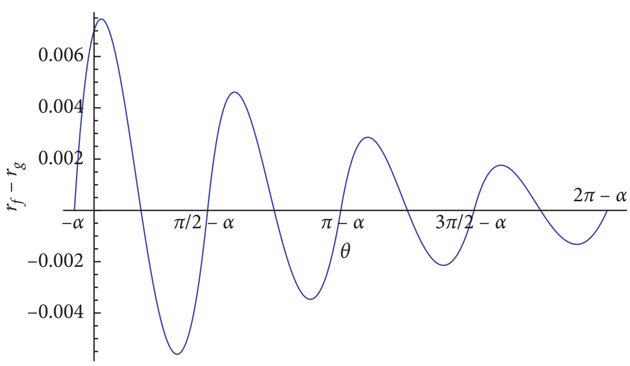

Figure 7: The difference of polar radii of the Fibonacci spiral and golden spiral ($a = 1$).

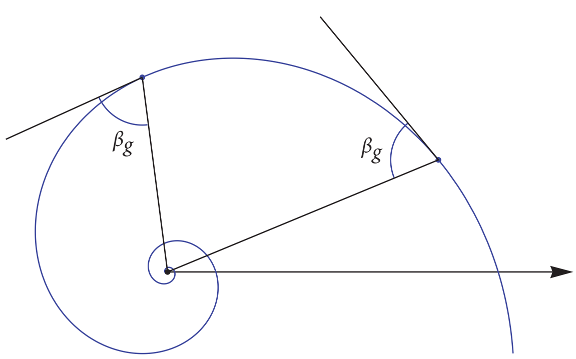

Figure 8: Arm-radius angle of the golden spiral.

angle θ are shown in the ordinary rectangle coordinate system in Figure 9, where we limit $-\alpha \le \theta \le 2\pi - \alpha$. The arm-radius angle β_g is a constant, while β_f oscillates continuously around β_g. At each corners, $\theta = -\alpha, (\pi/2) - \alpha, \pi - \alpha, \ldots$, the arm-radius angle β_f varies unsmoothly. MATHEMATICA code generating Figure 9 is attached in Appendix.

3.3. Curvatures. We rewrite the golden spiral in equation (30) to the parametric equation:

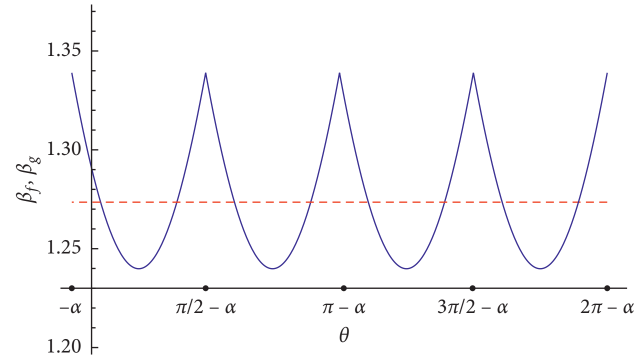

Figure 9: Arm-radius angles for the Fibonacci spiral (solid line) and golden spiral (dashed line).

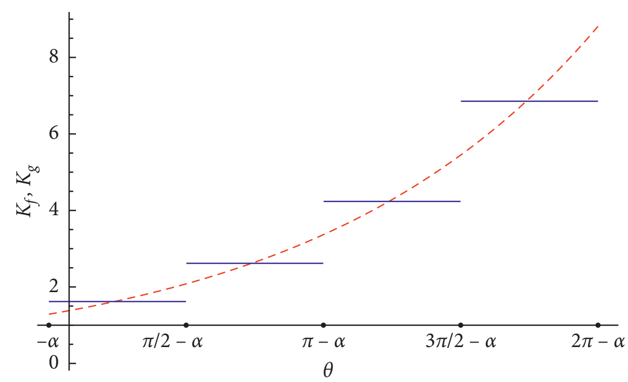

Figure 10: Curvatures of the Fibonacci spiral (solid line) and golden spiral (dashed line).

$$\begin{cases} x = \dfrac{a}{2-\lambda}\sqrt{1+\lambda^6}\,\lambda^{(2/\pi)(\theta+\alpha)}\cos\theta, \\[2ex] y = \dfrac{a}{2-\lambda}\sqrt{1+\lambda^6}\,\lambda^{(2/\pi)(\theta+\alpha)}\sin\theta. \end{cases} \tag{35}$$

Inserting the curvature formula

$$K_g = \frac{\left|x'(\theta)y''(\theta) - x''(\theta)y'(\theta)\right|}{\left(x'^2(\theta) + y'^2(\theta)\right)^{3/2}}, \tag{36}$$

we obtain the curvatures of the golden spiral

$$K_g = \frac{\pi(2-\lambda)}{a\sqrt{\left(1+\lambda^6\right)\left(\pi^2 + 4\ln^2\lambda\right)}\lambda^{(2/\pi)(\theta+\alpha)}}. \tag{37}$$

We take $a = 1$ and limit $-\alpha \le \theta \le 2\pi - \alpha$. The Fibonacci spiral has discontinuous curvatures K_f: $\lambda^{-1}, \lambda^{-2}, \lambda^{-3}$, and λ^{-4} for four quarter-circles, respectively, while the golden spiral has the continuous curvature in eqation (37). In Figure 10, curvatures of the Fibonacci spiral and golden spiral versus θ on the interval $-\alpha \le \theta \le 2\pi - \alpha$ are shown in an ordinary rectangle coordinate system.

4. Conclusion

We considered the golden rectangle and the related Fibonacci spiral and golden spiral. In Section 2, we gave the coordinates of the shrinkage points of a golden rectangle. Properties of shrinkage points were presented. In Section 3, we compared the Fibonacci spiral and golden spiral by examining their equations in polar coordinates, relationship of polar radii, and differences of arm-radius angles and curvatures. The golden spiral has a constant arm-radius angle and continuous curvature. As an approximation of the golden spiral, the Fibonacci spiral has continuous and smooth polar radius, cyclic varying arm-radius angle, and discontinuous curvature.

Appendix

MATHEMATICA code for Figure 9:

```
la = (Sqrt[5] − 1)/2;
betag = ArcCot[−2 Log[la]/Pi];
r = −a la^3/(2 − la) (Sin[th] − la Cos[th]) + a la/(2 − la)
Sqrt[la^4 (Sin[th] − la Cos[th])^2 + 6 la − 2];
x = r Cos[th];
y = r Sin[th];
OM = {x, y}; MT = {D[x, th], D[y, th]};
betaf = ArcCos[Abs[OM.MT]/Norm[OM]/Norm
[MT]];
al = ArcTan[2 la − 1];
f1 = Plot[{betaf, betag}, {th, −al, −al + Pi/2},
PlotStyle ⟶ {{}, {Dashed}}];
betaf2 = betaf/. th ⟶ (th − Pi/2);
f2 = Plot[{betaf2, betag}, {th, −al + Pi/2, −al + Pi},
PlotStyle ⟶ {{}, {Dashed}}];
betaf3 = betaf/. th ⟶ (th − Pi);
f3 = Plot[{betaf3, betag}, {th, −al + Pi, −al + 3 Pi/2},
PlotStyle ⟶ {{}, {Dashed}}];
betaf4 = betaf/. th ⟶ (th − 3 Pi/2);
f4 = Plot[{betaf4, betag}, {th, −al + 3 Pi/2, −al + 2 Pi},
PlotStyle ⟶ {{}, {Dashed}}];
Show[f1, f2, f3, f4, AxesOrigin ⟶ {0, 1.23},
PlotRange ⟶ {{−al, 6.15}, {1.2, 1.37}}, Ticks ⟶
{None}].
```

Data Availability

The data used to support the findings of this study are included within the article.

Conflicts of Interest

The author declares that he has no conflicts of interest.

Acknowledgments

This work was supported by the National Natural Science Foundation of China (no. 11772203) and the Natural Science Foundation of Shanghai (no. 17ZR1430000).

References

[1] A. Stakhov and B. Rozin, "On a new class of hyperbolic functions," *Chaos, Solitons & Fractals*, vol. 23, no. 2, pp. 379–389, 2005.

[2] M. Iosa, D. De Bartolo, G. Morone et al., "Gait phase proportions in different locomotion tasks: the pivot role of golden ratio," *Neuroscience Letters*, vol. 699, pp. 127–133, 2019.

[3] D. Chemla, D. Boulate, J. Weatherald et al., "Golden ratio and the proportionality between pulmonary pressure components in pulmonary arterial hypertension," *Chest*, vol. 155, no. 5, pp. 991–998, 2019.

[4] S. Ozturk, K. Yalta, and E. Yetkin, "Golden ratio: a subtle regulator in our body and cardiovascular system?," *International Journal of Cardiology*, vol. 223, no. 15, pp. 143–145, 2016.

[5] B. Herrmann, "Visibility in a pure model of golden spiral phyllotaxis," *Mathematical Biosciences*, vol. 301, pp. 185–189, 2018.

[6] Y. Gao, Z. Guo, Z. Song, and H. Yao, "Spiral interface: a reinforcing mechanism for laminated composite materials learned from nature," *Journal of the Mechanics and Physics of Solids*, vol. 109, pp. 252–263, 2017.

[7] G. G. Nyambuya, "On the gravitomagnetic origins of the anomalous flat rotation curves of spiral galaxies," *New Astronomy*, vol. 67, pp. 1–15, 2019.

[8] U. Lüttge and G. M. Souza, "The golden section and beauty in nature: the perfection of symmetry and the charm of asymmetry," *Progress in Biophysics and Molecular Biology*, vol. 146, pp. 98–103, 2019.

[9] L. D. G. Sigalotti and A. Mejias, "The golden ratio in special relativity," *Chaos, Solitons & Fractals*, vol. 30, no. 3, pp. 521–524, 2006.

[10] S. Böcker, "A golden ratio parameterized algorithm for cluster editing," *Journal of Discrete Algorithms*, vol. 16, pp. 79–89, 2012.

[11] S. K. Sen and R. P. Agarwal, "Golden ratio in science, as random sequence source, its computation and beyond," *Computers & Mathematics with Applications*, vol. 56, no. 2, pp. 469–498, 2008.

[12] H. T. Hu and J. M. Chen, "Maximization of fundamental frequencies of axially compressed laminated curved panels against fiber orientation," *Computers, Materials & Continua*, vol. 28, no. 3, pp. 181–212, 2012.

[13] C. C. Tsai and D. L. Young, "Using the method of fundamental solutions for obtaining exponentially convergent Helmholtz eigensolutions," *Computer Modeling in Engineering & Sciences*, vol. 94, no. 2, pp. 175–205, 2013.

[14] A. Stakhov and B. Rozin, "The golden shofar," *Chaos, Solitons & Fractals*, vol. 26, no. 3, pp. 677–684, 2005.

[15] I. Tanackov, I. Kovačević, and J. Tepić, "Formula for Fibonacci sequence with arbitrary initial numbers," *Chaos, Solitons & Fractals*, vol. 73, pp. 115–119, 2015.

[16] A. Stakhov, "The golden section, secrets of the Egyptian civilization and harmony mathematics," *Chaos, Solitons & Fractals*, vol. 30, no. 2, pp. 490–505, 2006.


Advances in
Operations Research
Advances in
Decision Sciences
Journal of
Applied Mathematics
The Scientific
World Journal
Journal of
Probability and Statistics
International
Journal of
Mathematics and
Mathematical
Sciences
Hindawi
Submit your manuscripts at
www.hindawi.com
Journal of
Optimization
International Journal of
Engineering
Mathematics
International Journal of
Analysis
Journal of
Complex Analysis
Advances in
Numerical Analysis
Mathematical Problems
in Engineering
International Journal of
Differential Equations
Discrete Dynamics in
Nature and Society
International Journal of
Stochastic Analysis
Journal of
Mathematics
Journal of
Function Spaces
Abstract and
Applied Analysis
Advances in
Mathematical Physics